

# Evidence for Resonance-Assisted Hydrogen Bonding from Crystal-Structure Correlations on the Enol Form of the $\beta$ -Diketone Fragment

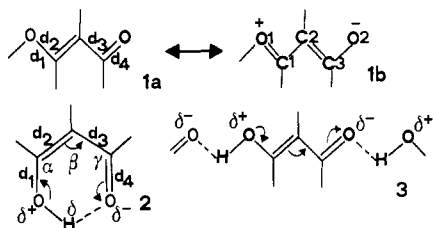
Gastone Gilli,\* Fabrizio Bellucci, Valeria Ferretti, and Valerio Bertolasi

Contribution from the Centro di Strutturistica Diffraattometrica and Dipartimento di Chimica, Università di Ferrara, 44100 Ferrara, Italy. Received May 4, 1987.

Revised Manuscript Received September 14, 1988

**Abstract:** The geometry variations caused by inter- and intramolecular hydrogen bond (HB) formation on the molecular fragment  $\text{acacH}$  ( $\text{HO-CR}=\text{CR}-\text{CR}=\text{O}$ ) contained in the enol form of acetylacetone and other related  $\beta$ -diketones and  $\beta$ -keto esters have been studied by crystal structure correlation methods on 25 X-ray or neutron crystallographically determined molecules containing such a fragment.  $\text{acacH}$  can form either a single intramolecular HB closing a 6-membered ring or intermolecular HBs connecting the groups head-to-tail in infinite linear arrays. Experimental data show that there is a strong correlation between the strength of the HB formed (measured by both the  $d_{\text{O}\cdots\text{O}}$  and  $d_{\text{O}\cdots\text{H}}$  values) and the delocalization of the system of conjugated double bonds. The effect is qualitatively interpreted in terms of a mechanism of synergistic interplay of resonance and HB formation which is called resonance-assisted hydrogen bonding (RAHB), and it is shown that the proposed model is in agreement with all present NMR and IR data and with the most recent ab initio quantum mechanical calculations reported for malonaldehyde. For more complex molecules a semiempirical model has been developed to evaluate both the energy of the HB formed ( $E_1$ ) and the height of the barrier for proton transfer ( $E_2$ ); with reference to water, where  $E_1 = 20$  and  $E_2 = 40$   $\text{kJ mol}^{-1}$ ,  $E_1$  and  $E_2$  are calculated to be 53.4 and 35  $\text{kJ mol}^{-1}$  in acetylacetone and 82.5 and 27.5  $\text{kJ mol}^{-1}$  in hexamethylacetylacetone, showing that very strong HB's with central hydrogen position are favored by substituents of relevant steric hindrance. These conclusions are generalized to take into account the possible role played by RAHB in a variety of heteroconjugated systems.

The ever growing number of structure determinations of molecular crystals by X-ray or neutron diffraction has contributed to the systematic comparison of the geometries of a molecular fragment in different crystal structures with the aim of extracting new, valuable chemical information, and in this connection, some specific techniques have been developed which are usually referred to as structure correlation methods.<sup>1</sup> In this paper such methods are applied to the  $\beta$ -diketone fragment in its enol form *1* (hereafter named  $\text{acacH}$  from acetylacetone) with the aim of understanding what happens to the fragment geometry when it is perturbed by intramolecular, 2, or intermolecular, 3, hydrogen bonding. The



specific  $\text{acacH}$  fragment has been chosen because  $\beta$ -diketones, over the years, have been of constant interest to inorganic, organic, and physical chemistry; the keto-enol equilibrium, the structures of both keto and enol forms, and the intramolecular  $\text{O}-\text{H}\cdots\text{O}$  hydrogen bond formed by the enol tautomer have been extensively studied by a remarkable variety of methods, including NMR, Raman, and IR spectroscopy, X-ray and neutron diffraction, and theoretical calculations, as recently reviewed in great detail by Emsley.<sup>2</sup> Starting from Emsley's considerations and conclusions, the idea of this work came from the empirical observation that a greater delocalization of the  $\pi$ -conjugated system occurs in the  $\text{HO-CR}=\text{CR}-\text{CR}=\text{O}$  ( $\text{acacH}$ ) fragment when it forms either intramolecular or infinite-chain intermolecular hydrogen bonding.<sup>3</sup> The nature and the entity of the effect is shown in Table I. Here the *standard* distances are those tabulated<sup>1a,1e</sup> for pure single and double bonds, while the *unperturbed* ones have been determined as an average of nine fragments (see next paragraph) that have

Table I. Selected Geometries for the  $\text{acacH}$  Fragment<sup>a</sup>

|                | $d_1$     | $d_2$     | $d_3$     | $d_4$     | % $1b^b$ |
|----------------|-----------|-----------|-----------|-----------|----------|
| standard       | 1.37      | 1.33      | 1.48      | 1.20      | 0        |
| unperturbed    | 1.353 (4) | 1.344 (3) | 1.454 (5) | 1.225 (3) | 13       |
| extreme        |           |           |           |           |          |
| perturbations  |           |           |           |           |          |
| intermolecular | 1.316 (2) | 1.372 (2) | 1.431 (2) | 1.238 (2) | 29       |
| HB (3)         |           |           |           |           |          |
| intramolecular | 1.281 (4) | 1.398 (4) | 1.410 (4) | 1.279 (4) | 48       |
| HB (2)         |           |           |           |           |          |

<sup>a</sup> Distances are in Å and esd's are in parentheses.  $d_{1-4}$  are defined in 1a and 2. <sup>b</sup>  $1b\%$  = percent contribution of the polar form 1b to the fundamental state according to Pauling's formula of bond order.<sup>4</sup>

not been "perturbed" by hydrogen bond formation. The *unperturbed* geometry can be described as a 87:13 mixture of the resonance forms 1a and 1b to the fundamental state according to the Pauling's formula of bond order.<sup>4</sup> However, when  $\text{acacH}$  forms, in molecular crystals, intramolecular (2), or chain intermolecular (3) hydrogen bonds,  $d_1$ ,  $d_2$ ,  $d_3$ , and  $d_4$  distances undergo changes which are consistent with an increased contribution of the polar form 1b to the limits of 29 or 48% for the inter- or intramolecular case, respectively.

(1) Bent, H. A. *Chem. Rev.* **1968**, *68* 587. Buergi, H. B. *Inorg. Chem.* **1973**, *12*, 2321. Buergi, H. B.; Dunitz, J. D.; Shefter, E. *J. Am. Chem. Soc.* **1973**, *95*, 5065. Buergi, H. B. *Angew. Chem., Int. Ed. Engl.* **1975**, *14*, 460. Dunitz, J. D. *X-ray Analysis and the Structure of Organic Molecules*; Cornell University Press: Ithaca, 1979. Buergi, H. B.; Dunitz, J. D. *Acc. Chem. Res.* **1983**, *16*, 153. Buergi, H. B. Static and Dynamic Implications of Precise Structural Informations. Reports of the 11th International School of Crystallography, Erice, Italy, 1985; pp 245-266.

(2) Emsley, J. *Struct. Bonding* **1984**, *57*, 147.

(3) Gilli, G.; Bellucci, F.; Ferretti, V.; Bertolasi, V. Proceedings of the 10th E.C.M. Pre-Meeting Symposium on Organic Crystal Chemistry, Poznań, Poland, 1986; pp 45-46.

(4) Pauling's formula of bond order (Pauling, L. *J. Am. Chem. Soc.* **1947**, *69*, 542) is  $d(1) - d(n) = -c \log n$ , where  $n$  is the bond order,  $d(1)$  and  $d(n)$  are the distances of single and multiple bond, and  $c = [d(1) - d(2)]/\log 2$  is a constant to be evaluated. In the present case (Table I) standard single and double bond distances<sup>1a,e</sup> are  $d_1 = \text{C}(\text{sp}^2)-\text{O} = 1.37$ ,  $d_2 = \text{C}(\text{sp}^2)=\text{C}(\text{sp}^2) = 1.33$ ,  $d_3 = \text{C}(\text{sp}^2)-\text{C}(\text{sp}^2) = 1.48$ , and  $d_4 = \text{C}(\text{sp}^2)=\text{O} = 1.20$  Å, and  $c$  is easily calculated to be 0.565 and 0.498 Å for C-O and C-C bonds, respectively.

\* Address correspondence to Prof. Gastone Gilli, Dipartimento di Chimica, Università di Ferrara, Via L. Borsari, 46, 44100 Ferrara, Italy.

Table II. Selected Internuclear Distances for acacH Fragments<sup>a</sup>

|                  | $d_1$ | $d_2$ | $d_3$ | $d_4$ | esd               | $q_1$  | $q_2$  | $Q$    | $d_{O\cdots O}$ | $d_{O\cdots H}$   | $d_{H\cdots O}$   | esd               | $\lambda$ |
|------------------|-------|-------|-------|-------|-------------------|--------|--------|--------|-----------------|-------------------|-------------------|-------------------|-----------|
| 1                | 1.290 | 1.390 | 1.398 | 1.297 | 0.013             | 0.007  | -0.008 | -0.001 | 2.481           | <i>f</i>          |                   |                   | 0.50      |
| 2 <sup>b</sup>   | 1.281 | 1.398 | 1.410 | 1.279 | 0.004             | -0.002 | -0.012 | -0.014 | 2.485           | 1.24              | 1.32              | 0.01              | 0.52      |
| 2'               | 1.294 | 1.376 | 1.401 | 1.276 | 0.003             | -0.018 | -0.025 | -0.043 | 2.498           | 1.18              | 1.40              | 0.03              | 0.57      |
| 3                | 1.313 | 1.391 | 1.397 | 1.288 | 0.004             | -0.025 | -0.006 | -0.031 | 2.456           | 1.12              | 1.37              | 0.05              | 0.55      |
| 4                | 1.304 | 1.382 | 1.408 | 1.287 | 0.002             | -0.017 | -0.026 | -0.043 | 2.460           | 1.22              | 1.28              | 0.03              | 0.57      |
| 4'               | 1.302 | 1.377 | 1.404 | 1.277 | 0.006             | -0.025 | -0.027 | -0.052 | 2.468           | <i>g</i>          |                   |                   | 0.58      |
| 4'' <sup>b</sup> | 1.311 | 1.391 | 1.422 | 1.273 | 0.004             | -0.038 | -0.031 | -0.069 | 2.459           | 1.16              | 1.36              | 0.01              | 0.61      |
| 5                | 1.306 | 1.380 | 1.408 | 1.279 | 0.003             | -0.027 | -0.028 | -0.055 | 2.470           | 1.15              | 1.37              | 0.03              | 0.59      |
| 6                | 1.316 | 1.384 | 1.416 | 1.278 | 0.004             | -0.038 | -0.032 | -0.070 | 2.455           | 1.20              | 1.32              | 0.04              | 0.61      |
| 7                | 1.312 | 1.383 | 1.415 | 1.253 | 0.009             | -0.059 | -0.032 | -0.091 | 2.458           | <i>g</i>          |                   |                   | 0.64      |
| 8                | 1.303 | 1.388 | 1.447 | 1.266 | 0.004             | -0.037 | -0.059 | -0.096 | 2.417           | 1.22              | 1.35              | 0.04              | 0.65      |
| 9 <sup>c</sup>   | 1.316 | 1.372 | 1.431 | 1.238 | 0.002             | -0.078 | -0.059 | -0.137 | 2.575           | 0.97              | 1.61              | 0.02              | 0.71      |
| 10               | 1.327 | 1.360 | 1.444 | 1.267 | 0.017             | -0.060 | -0.084 | -0.144 | 2.461           | 1.17 <sup>b</sup> | 1.39 <sup>b</sup> | 0.02 <sup>b</sup> | 0.72      |
| 11               | 1.320 | 1.382 | 1.452 | 1.244 | 0.003             | -0.076 | -0.070 | -0.146 | 2.522           | 1.01              | 1.62              | 0.03              | 0.73      |
| 11'              | 1.327 | 1.379 | 1.453 | 1.249 | 0.003             | -0.078 | -0.074 | -0.152 | 2.517           | 1.14              | 1.45              | 0.03              | 0.74      |
| 12               | 1.312 | 1.384 | 1.442 | 1.218 | 0.006             | -0.094 | -0.058 | -0.152 | 2.545           | 0.97              | 1.66              | 0.08              | 0.74      |
| 13               | 1.346 | 1.372 | 1.442 | 1.236 | 0.009             | -0.110 | -0.070 | -0.180 | 2.527           | <i>g</i>          |                   |                   | 0.78      |
| 14               | 1.329 | 1.367 | 1.467 | 1.234 | 0.004             | -0.095 | -0.100 | -0.195 | 2.547           | <i>g</i>          |                   |                   | 0.80      |
| 15               | 1.345 | 1.354 | 1.451 | 1.245 | 0.004             | -0.100 | -0.097 | -0.197 | 2.554           | 0.97              | 1.69              | 0.03              | 0.81      |
| 16 <sup>c</sup>  | 1.334 | 1.341 | 1.438 | 1.228 | 0.007             | -0.106 | -0.097 | -0.203 | 2.600           | <i>g</i>          |                   |                   | 0.82      |
| 16' <sup>c</sup> | 1.326 | 1.335 | 1.436 | 1.219 | 0.003             | -0.107 | -0.101 | -0.208 | 2.600           | 0.97              | 1.63              | 0.04              | 0.82      |
| 17               | 1.332 | 1.347 | 1.448 | 1.223 | 0.007             | -0.109 | -0.101 | -0.210 | 2.564           | 0.97              | 1.69              | 0.08              | 0.83      |
| 18               | 1.344 | 1.350 | 1.445 | 1.223 | 0.005             | -0.121 | -0.095 | -0.216 | 2.614           | 0.97              | 1.75              | 0.04              | 0.84      |
| 19               | 1.352 | 1.342 | 1.448 | 1.239 | 0.004             | -0.113 | -0.106 | -0.219 | 2.665           | <i>g</i>          |                   |                   | 0.84      |
| 20               | 1.338 | 1.352 | 1.455 | 1.216 | 0.001             | -0.122 | -0.103 | -0.225 | 2.615           | 0.97              | 1.74              | 0.03              | 0.85      |
| U <sup>d</sup>   | 1.353 | 1.344 | 1.454 | 1.225 | 0.01 <sup>b</sup> | -0.128 | -0.110 | -0.238 |                 |                   |                   |                   | 0.87      |
| S <sup>e</sup>   | 1.37  | 1.33  | 1.48  | 1.20  |                   | -0.17  | -0.15  | -0.32  |                 |                   |                   |                   | 1         |

<sup>a</sup> Distances and esd's are in Å; references can be found in Table S3, internuclear angles are in Table S4 and the structures of 1–20 are in Table S5 (all deposited<sup>8</sup>).  $Q = q_1 + q_2$  and  $\lambda = (1 - Q/3.320)/2$  (see text). <sup>b</sup> Structure determined by neutron diffraction. <sup>c</sup> Intermolecular hydrogen bonding (2). <sup>d</sup> Unperturbed geometry. <sup>e</sup> Standard geometry. <sup>f</sup> Values not reported. <sup>g</sup> Values not considered. <sup>h</sup> Esd of the weighted average of nine structures.

### Data Retrieval

Two crystal structures have been determined in our laboratory<sup>5</sup> (compounds 3 and 5 of Table II) whereas all other crystallographic data have been retrieved from the Cambridge Structural Database (1986 release)<sup>6</sup> by using the following criteria.

(a) **Reliability:**  $R < 0.10$  (neutrons) or  $< 0.07$  (X-rays),  $d_{C-C} < 0.015$  Å, no disorder in the non-hydrogen atoms, no acacH fragments located on crystallographic symmetry elements to avoid hydroxyl hydrogens in apparent central O...H...O position caused by disorder.<sup>7</sup>

(b) **Structural Requirements.** To avoid unwanted geometry perturbations, all acacH fragments carrying other heteroatoms were excluded, with the exception of the OR group at C<sub>3</sub> (i.e.  $\beta$ -keto esters were included) and of one SSSR group at C<sub>2</sub> (compound 10 of Table II). Fragments where C<sub>1</sub>, C<sub>2</sub>, or C<sub>3</sub> atoms were part of an aromatic ring were not taken into account.

(c) **Hydrogen Bonds.** All structures where acacH forms other hydrogen bonds in addition to those of 2 or 3 were excluded.

(d) **Unperturbed Sample.** The same limitations as in (a) and (b) plus R = alkyl instead of H were adopted. With these limitations nine unperturbed acacR fragments were retrieved (Table S1<sup>8</sup>); their weighted average distances (end of Table II) were considered to represent the fragment geometry when not perturbed by hydrogen bond formation.

Moreover three type 3 and 22 type 2 acacH fragments were observed; for each one  $d_1$ ,  $d_2$ ,  $d_3$ ,  $d_4$ ,  $d_{O1-H}$ ,  $d_{O1\cdots O2}$ , and  $d_{O2\cdots H}$  distances were registered (Table II) and their references and bond

angles are reported in Tables S3 and S4.<sup>8</sup> All X-ray O–H distances were corrected according to a method used by Taylor and Kennard<sup>9</sup> for a similar situation. Determined  $d_{O-H}$  values have been corrected by displacing the H atom along the O–H bond at 0.97 Å when  $d_{O-H} \leq 0.97$  Å, but leaving distances  $> 0.97$  Å unchanged.<sup>10</sup> Only two full refinements of neutron data (compounds 2 and 4') and a partial one (compound 10) have been reported so far, so mostly H positions from X-ray scattering are used here; to increase reliability, H positions were kept only for structures having  $R < 0.065$  and a ratio of the number of independent reflections/number of refined parameters  $> 5.3$ .

Molecular structures determined by gas-phase electron-diffraction (ged) methods and microwave (MW) spectroscopy were reviewed as well. In the only accurate MW structure (malonaldehyde)<sup>11</sup> the position of the hydroxyl H atom was not experimentally determined but calculated from neutron diffraction data. As far as ged structures are concerned, most of them<sup>12</sup> assume C<sub>2v</sub> symmetry and are of little use here; only the most recent one, that of acetylacetone,<sup>13</sup> reports the complete molecular geometry.

### Structure Correlations

**Symmetry Coordinates.** Actual  $d_1$ – $d_4$  values were considered to be antisymmetrical in-plane vibrations belonging to the B<sub>1</sub> irreducible representation of the C<sub>2v</sub> geometry 4. The corresponding symmetry coordinates are  $q_1 = d_4 - d_1$  and  $q_2 = d_2 - d_3$ .

(9) Taylor, R.; Kennard, O. *Acta Crystallogr., Sect. B* 1983, 39, 133.

(10) To check this correction procedure we have retrieved from the Cambridge Structural Database<sup>6</sup> 109 couples of  $d_{O-H}$  values determined both by neutron (N) and X-ray diffraction (X). The scatter plot  $d_{O-H}(N)$  vs  $d_{O-H}(X)$  has definitely the expected form, i.e. a slope of zero in the interval  $0.80 \leq d_{O-H}(X) \leq 0.97$  Å and a slope of one for  $d_{O-H}(X) > 0.97$  Å (paper in preparation).

(11) Baughcum, S. L.; Duerst, R. W.; Rowe, W. F.; Smith, Z.; Bright Wilson, E. J. *Am. Chem. Soc.* 1981, 103, 6296. Relevant parameters are  $d_1 = 1.320$ ,  $d_2 = 1.348$ ,  $d_3 = 1.454$ ,  $d_4 = 1.234$ ,  $q_1 = -0.086$ ,  $q_2 = -0.106$ ,  $Q = -0.192$ ,  $d_{O\cdots O} = 2.553$ – $2.574$ , and  $d_{O-H} = 0.969$  (assumed) Å.

(12) Lowrey, A. H.; George, C.; D'Antonio, P.; Karle, J. *J. Am. Chem. Soc.* 1971, 93, 6399.

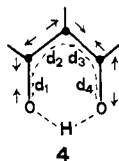
(13) Iijima, K.; Ohnogi, A.; Shibata, S. *J. Mol. Struct.* 1987, 156, 111. Relevant parameters are  $d_1 = 1.319$  (3),  $d_2 = 1.382$  (7),  $d_3 = 1.430$  (8),  $d_4 = 1.243$  (2),  $q_1 = -0.076$ ,  $q_2 = -0.048$ ,  $Q = -0.124$ ,  $d_{O\cdots O} = 2.512$  (8),  $d_{O-H} = 1.049$  (15) Å.

(5) Gilli, G.; et al., paper in preparation.

(6) Allen, F. H.; Bellard, S.; Brice, M. D.; Cartwright, B. A.; Doubleday, A.; Higgs, H.; Hummelink, T.; Hummelink-Peters, B. G.; Kennard, O.; Motherwell, W. D. S.; Rogers, J. R.; Watson, D. G. *Acta Crystallogr., Sect. B* 1979, 35, 2331.

(7) The only case of *m* crystallographic symmetry reported refers to the structure of bis(*m*-bromobenzoyl)methane (Williams, D. E.; Dumke, W. L.; Rundle, R. E. *Acta Crystallogr.* 1962, 15, 627).

(8) Tables S1–S5 and Figure S1 have been deposited as supplementary material and contain respectively: selected interatomic distances for the unperturbed acacH fragment with references (Table S1), structures for the compounds of Table S1 (Table S2), references for compounds of Table S5 (Table S3), selected intermolecular angles for acacH fragments of Table II (Table S4), structures for all molecules carrying the acacH fragment taken into account (Table S5), and a  $d_{O-H}$  and  $d_{O\cdots O}$  vs  $d_{O\cdots O}$  scatterplot (Figure S1).



**$q_1$  versus  $q_2$  Correlation.** The scatter plot of all the data of Table II in the  $q_1, q_2$  space is reported in Figure 1. The plot has central symmetry as data can be plotted twice according to the equivalence of the enoketonic (EK) and ketoenolic (KE) forms in fragment 4, and its center corresponds to the totally delocalized  $\pi$ -bond system. The extreme full squares of the curve (marked EK and KE) are representative of the enoketonic and ketoenolic geometries for hypothetical *standard* pure single and double bond distances (Table I); the two stars have a similar meaning but with reference to the geometry *unperturbed* by hydrogen bonding. The distribution of the experimental points shows that any perturbation can be observed up to the full delocalization. The dashed line connecting EK and KE squares represents the equation  $q_2 = 0.882q_1$ , calculated from the values of  $q_1 = -0.17$  and  $q_2 = -0.15$  for the *standard* geometry S of Table II and it is seen to reasonably fit the experimental points.

As  $q_1$  and  $q_2$  appear to be linearly dependent, a single coordinate  $Q = q_1 + q_2$  can be used,  $Q = 0$  corresponding to the fully  $\pi$ -delocalized structure and  $Q = -0.320$  or  $+0.320$  Å to the completely  $\pi$ -localized EK or KE forms, respectively. Alternatively, as the perturbation of the conjugated system substantially mixes the EK and KE geometries, the mixing can be described by a coupling parameter,  $\lambda$ .<sup>14</sup> The state of the fragment is expressed as  $\lambda(\text{EK}) + (1 - \lambda)(\text{KE})$  with  $\lambda = (1 - Q/0.320)/2$  and  $\lambda = 1, 0.5$ , and  $0$ , corresponding to the  $\pi$ -localized EK and the fully delocalized and localized KE forms, respectively. The data of Table II are approximately arranged in order of increasing  $Q$  and  $\lambda$  values.

**$d_{\text{O}\cdots\text{O}}$  versus  $Q$  Correlation.** The scatter plot of  $d_{\text{O}\cdots\text{O}}$ , the contact distance between the two oxygens implied in the  $\text{O}_1\text{---H}\cdots\text{O}_2$  hydrogen bond, and  $Q = q_1 + q_2$  for all acacH fragments of Table II is shown in Figure 2. The plot is symmetric with respect to the displacements from the delocalized structure having  $Q = 0$  and  $\lambda = 0.5$ . Very short values of  $d_{\text{O}\cdots\text{O}}$  are associated with small values of  $|Q|$ , that is with strong  $\pi$ -bond delocalization. The relevance of the shortening can be evaluated by taking into account that the  $d_{\text{O}\cdots\text{O}}$  distance is typically 2.76 Å in ice and that the average value of this quantity in  $\text{R}_3\text{C}\text{---OH}\cdots\text{O}=\text{CR}_2$  contacts is  $2.80 \pm 0.08$  Å.<sup>15</sup>

**$d_{\text{O}\cdots\text{H}}$  and  $d_{\text{H}\cdots\text{O}}$  Distances.** An analysis of the correlation among the covalent  $d_{\text{O}\cdots\text{H}}$  and contact  $d_{\text{O}\cdots\text{H}}$  distances and different values of the contact  $d_{\text{O}\cdots\text{O}}$  distances for the structures of Table II, whose refined H positions are known, is reported in Figure S1.<sup>8</sup> It shows that in compounds of Table II there is no evidence of fully symmetrical  $\text{O}\cdots\text{H}\cdots\text{O}$  bonds, suggesting that, at least in the crystalline state, the enolic proton of the acacH fragment experiences, for the full range of  $d_{\text{O}\cdots\text{O}}$  values, a double minimum potential. This result is in touch with a variety of experimental IR, Raman, and NMR data obtained in solution and in gas or solid state and reviewed by Emsley<sup>2,16</sup> and is in agreement with a recent study<sup>17</sup> which has shown that the HOMO-LUMO configurational interaction in 2 would cause a second-order Jahn-Teller distortion of a symmetrical  $\text{O}\cdots\text{H}\cdots\text{O}$  hydrogen bond even in a molecule of potential  $C_{2v}$  symmetry, e.g. in the enolic form of dibenzoylmethane (compound 4 of Table II). Moreover, present data do not suggest the presence of a disordered double position of the H atom in spite of the fact that proton tunneling has been observed in malonaldehyde in the gas phase<sup>11</sup> and that proton disorder has

(14) Mezei, M.; Beveridge, D. L. *Anal. N.Y. Acad. Sci.* **1986**, *82*, 1. Kirkwood, J. D. In *Theory of Liquids*; Adler, B. J., Ed.; Gordon and Breach: New York, 1968.

(15) Value obtained by averaging the 29  $d_{\text{O}\cdots\text{O}}$  values of  $\text{R}_3\text{COH}\cdots\text{O}=\text{CR}_2$  inter- or intramolecular hydrogen bonds ( $\text{R} = \text{H}$  or alkyl) published in the years 1984-1985 in *Acta Crystallographica*.

(16) Emsley, J. *Chem. Soc. Rev.* **1980**, *9*, 91.

(17) Haddon, R. C. *J. Am. Chem. Soc.* **1980**, *102*, 1807.

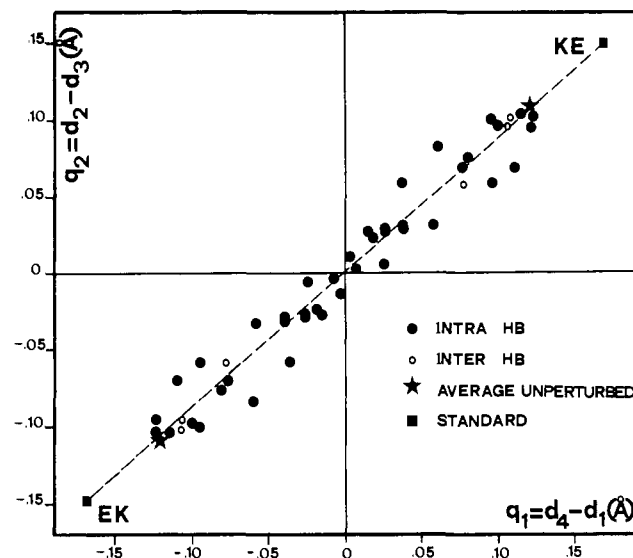


**Figure 1.** Scatter plot in the  $(q_1, q_2)$  space for all data of Table II. The full squares and stars refer to the *standard* and *unperturbed* acacH geometries, respectively; full and open circles refer to acacH geometries perturbed by intra- and intermolecular hydrogen bonds, respectively.

been seen in a number of crystals.<sup>18</sup>

**Interatomic Angles.** Let us call  $\alpha$ ,  $\beta$ , and  $\gamma$  respectively the angles  $\text{O}_1\text{---C}_1=\text{C}_2$ ,  $\text{C}_1=\text{C}_2\text{---C}_3$ , and  $\text{C}_2\text{---C}_3=\text{O}_2$  and  $\delta$  the angle  $\text{O}_1\text{---H}\cdots\text{O}_2$ . As for  $\delta$ , the data of Table II and S4<sup>8</sup> show that in the intramolecular hydrogen bond (2) this angle is almost independent of the  $d_{\text{O}\cdots\text{O}}$  distance with an average value of  $149$  [5] $^\circ$  and that in the intermolecular case (3) this angle takes the rather different value of  $173$  [4] $^\circ$ . Analysis of the  $\alpha$ ,  $\beta$ , and  $\gamma$  values is complicated by the variety of chemical situations in which the fragment is found (Table S5).<sup>8</sup> A comparison can be carried out by taking into account only intramolecular hydrogen bonded fragments (2) where the  $\text{C}=\text{C}\text{---C}$  group is not part of a ring with less than six members (compounds 1-8, 10, 12-15, 17, 18, 20). The average values are as follows:

| $d_{\text{O}\cdots\text{O}}$ range | 2.40-2.51  | 2.52-2.59  | 2.60-2.70 | full range |
|------------------------------------|------------|------------|-----------|------------|
| means                              | 120.5 [8]  | 123.8 [10] | 125.3 [4] | 122.1 [20] |
|                                    | 120.5 [15] | 118.0 [10] | 119.1 [3] | 119.5 [12] |
|                                    | 120.4 [10] | 124.1 [10] | 124.3 [6] | 122.0 [20] |

and show that, on average, the shortening of the  $\text{O}\cdots\text{O}$  distance

(18) Enolic proton tunnelling has been actually observed in some molecules carrying the acacH fragment, e.g. in malonaldehyde by microwave spectroscopy<sup>11</sup> and naphthazarin by  $^1\text{H}$  and  $^{13}\text{C}$  NMR (Moore, R. E.; Schuer, P. *J. J. Org. Chem.* **1966**, *31*, 3272. Dumas, J. M.; Cohen, A.; Gomet, M. *Bull. Soc. Chim. Fr.* **1972**, 1340. de la Vega, J. R.; Bush, J. H.; Schauble, J. H.; Kunze, K. L.; Haggert, B. E. *J. Am. Chem. Soc.* **1982**, *104*, 3295. Kobayashi, M.; Terni, Y.; Turi, K. *Tetrahedron Lett.* **1976**, 619) and IR spectroscopy (Braton, S.; Strolbuch, F. *J. Mol. Struct.* **1980**, *61*, 409). A theoretical study (De la Vega, J. R. *Acc. Chem. Res.* **1982**, *15*, 185) has shown that proton tunnelling is quenched by geometrical dissymmetries and can occur only in molecules having  $C_s$  symmetry with respect to the plane perpendicular to the mean plane of the fragment. Such a requirement is difficult to be fulfilled even for symmetrical molecules in crystals in consequence of small incidental conformational differences, but they can be met when the molecule lies astride a crystallographic symmetry plane; in such a case, however, static disorder would be indistinguishable from proton tunnelling (see for instance ref 7). The analysis of the order  $\leftrightarrow$  disorder transition of naphthazarine C at 110 K (by X-ray and neutron diffraction; Herstein, F. H.; Kapon, M.; Reinsner, G. M.; Lehman, M. S.; Kress, R. B.; Wilson, R. B.; Shian, W.-I.; Duesler, E. N.; Paul, I. C.; Curtin, D. Y. *Proc. R. Soc. London, A* **1985**, *A399*, 295) seems to indicate that disorder in the enolic proton positions can be associated with molecules where the acacH fragment forms both intra- (2) and intermolecular (3) hydrogen bonds (a case excluded here). Similar conclusions have been drawn by Saenger (Betsel, C.; Saenger, W.; Hingety, B. E.; Brown, G. M. *J. Am. Chem. Soc.* **1984**, *106*, 7545. Saenger, W. *Principles of Nucleic Acid Structure*; Springer-Verlag: New York, 1984) mainly on the grounds of the neutron-diffraction structure of  $\beta$ -cyclodextrine undecahydrate, where "flip-flop"  $\text{O}\cdots\text{H}\cdots\text{O} = \text{O}\cdots\text{H}\cdots\text{O}$  hydrogen bonds were found to be associated with extended "homodromic, antidromic and heterodromic" circular systems of hydrogen bonds where "the transition from one state into the other is not by tunnelling of the hydrogen... but rather by rotation of hydroxyl groups".

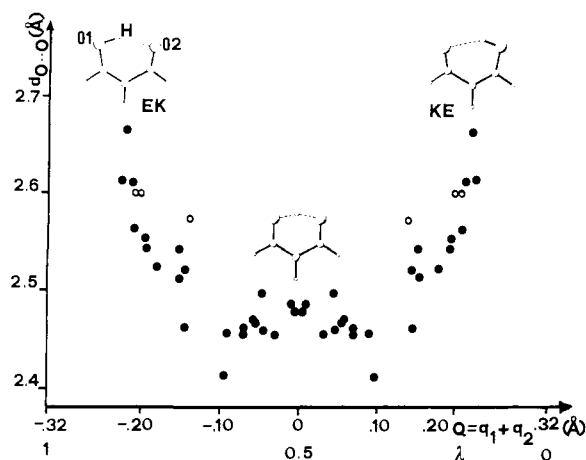


**Figure 2.** Scatter plot in the ( $d_{\text{O}\cdots\text{O}}$ ,  $Q$ ) space for all data of Table II. Full and open circles indicate acacH fragments forming intra- and intermolecular hydrogen bonds, respectively.

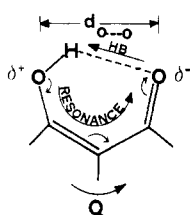


**Figure 3.** A graphical scheme of the RAHB model.

consequent to hydrogen-bond strengthening is mainly achieved by the narrowing of both  $\alpha$  and  $\gamma$  whereas  $\beta$  remains practically unchanged.

#### Data Interpretation

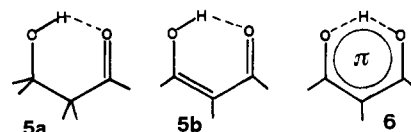
**A Qualitative Model.** The observed correlations are in agreement with the qualitative interpretation sketched in Figure 3. Firstly, assuming a single C–C instead of a double C=C bond, the hydrogen bond formed will be the balance among different factors, that is, the energy of the hydrogen bond itself,  $E_{\text{HB}}$ , plus the ring energies, such as those of bond angle bending and van der Waals 1–4 interactions,  $E_{\text{vdw}}$ , due to the  $R_1$ – $R_3$  substituents. Now, by reestablishing the double C=C bond, the resonance  $1a \leftrightarrow 1b$  will cause a shift of electrons from left to right (Figure 3) which will stop when  $E_{\text{RES}} + E_{\text{BP}}$  reaches a minimum, where  $E_{\text{RES}}$  is the energy of delocalization of the  $\pi$  system and  $E_{\text{BP}}$  is the bond polarization energy needed to dissociate the partial charges on the terminal oxygens. These have the correct sign for strengthening the hydrogen bond with consequent shortening of  $d_{\text{O}\cdots\text{O}}$  and lengthening of  $d_{\text{O}\cdots\text{H}}$ . The proton movement corresponds to a vacancy going to the right or to a negative charge going to the left, and thus the total effect is the annihilation through hydrogen-bond transmission of the partial charges generated initially by resonance, so allowing an increased contribution of the polar form  $1b$  and a further strengthening of the hydrogen bond, this imaginary process going on until the minimum of the function  $E = E_{\text{HB}} + E_{\text{RES}} + E_{\text{BP}} + E_{\text{vdw}}$  is attained.

This strengthened hydrogen bond may be called a *resonance assisted hydrogen bond* (RAHB). It is phenomenologically associated with the intercorrelation of  $Q$  or  $\lambda$  (both measuring the  $\pi$ -system delocalization) with the variations of the O $\cdots$ O or O–H distances (both measuring the strength of the hydrogen bond). The hydrogen bonding scheme is usually intramolecular, 2, but may be intermolecular, 3, as well, and in this second case the effect of hydrogen-bonding strengthening appears to be smaller. In a sense RAHB can be conceived as a feedback mechanism which maintains zero partial charges on the two opposite oxygens by quenching the increase due to resonance with a decrease caused by the proton shift.

An alternative exposition of the RAHB model can be as follows.<sup>19</sup> The hydrogen bond is formed by donation of the *in-plane*

( $\pi'$ ) lone pair of the carbonyl oxygen in Figure 3, whereas resonance involves donation of the *out-of-plane* ( $\pi$ ) lone pair on the enol to the carbonyl oxygen. The basis energy of the  $\pi'$  lone pair orbital is *increased*, owing to the *decreased* electronegativity of the oxygen resulting from  $\pi$  resonance. Hence the  $\pi'$  lone pair becomes a better electron donor and a stronger hydrogen-bond acceptor.

Several independent data suggesting a relationship between hydrogen-bond strengthening and  $\pi$  conjugation in  $\beta$ -diketones have been reported in the past. The most convincing proof is probably the strict proportionality of  $^1\text{H}$  NMR downfield chemical shift of the enolic proton (a common indicator of the hydrogen-bond strength) and of the IR frequency of the O–D out-of-plane vibration,  $\nu(\text{OD})$  (a measure of  $\pi$  conjugation),<sup>20a</sup> on one side, and the increase of the IR  $\nu(\text{OH})$  stretching frequency when the hydrogen bond forms a ring with a conjugated  $\pi$  system on the other. By this last method Kopleva and Shigorin<sup>20b</sup> estimated that the intramolecular hydrogen bond was stronger in the enolic form of dibenzoylmethane **5b** than in **5a** by some 60 kJ mol<sup>-1</sup> while the integrated intensities of the stretching bands were strictly comparable, a behavior which is in total disagreement with what is observed in common O–H $\cdots$ O bonds, where the band intensities increase linearly with the bond energies. These findings were not properly interpreted by a previous theory based on the supposed benzenoid character of ring **6**,<sup>21a,21b</sup> which is characterized by a



strong and centered hydrogen bond (see also the review by Pimentel and McClellan<sup>21c</sup>). It seems clear that any evidence of a noncentered proton discredits this theory as it is actually done not only with the data of Table II but also with the IR and Raman evidence that molecules obtainable by symmetrical substitution of the acacH fragment have  $C_3$  and never  $C_{2v}$  symmetry.<sup>2,22</sup> On the contrary, the RAHB model does not have difficulties in dealing with noncentered hydrogen positions and can explain the apparent paradox of a very strong hydrogen bond associated with abnormally small  $\nu(\text{OH})$  stretching band intensities<sup>19</sup> reported above in terms of the damping of the transition moment of the  $\nu(\text{OH})$  vibration through the feedback of the  $\pi$ -conjugated system. Several ab initio quantum mechanical studies on intramolecularly hydrogen-bonded malonaldehyde, with either partial or complete optimization of the molecular geometry, are reported in the literature<sup>23,24</sup> and are to be compared with its microwave-determined structure<sup>11</sup> (relevant parameters:  $Q = -0.192$ ,  $\lambda = 0.80$ , and  $d_{\text{O}\cdots\text{O}} = 2.553$ – $2.574$  Å,  $d_{\text{O}\cdots\text{H}}$  not determined). The results consistently indicated that SCF or Hartree–Fock approximation is incapable of giving the correct geometry of malonaldehyde; it has also been shown<sup>24</sup> that the most extended basis sets (Huzinaga–Dunning's<sup>25</sup>

(19) This interpretation has been suggested by one of the referees. A similar effect has been discussed in a different context (Staley, S. W.; Norden, T. D.; Taylor, W. H.; Harmony, M. D. *J. Am. Chem. Soc.* **1987**, *109*, 7641.)

(20) Ogoshi, H.; Yoshida, Z. *Chem. Commun.* **1970**, 176. Kopleva, T. S.; Shigorin, D. N. *Russ. J. Phys. Chem.* **1974**, *48*, 312.

(21) Vinogradov, S. N.; Linnel, R. H. *Hydrogen Bonding*; van Nostrand Reinhold: New York, 1971. Williams, D. E.; Dumke, W. L.; Rundle, R. E. *Acta Crystallogr.* **1962**, *15*, 627. Pimentel, G. C.; McClellan, A. L. *The Hydrogen Bond*; Freeman: San Francisco, 1960; pp 239–240.

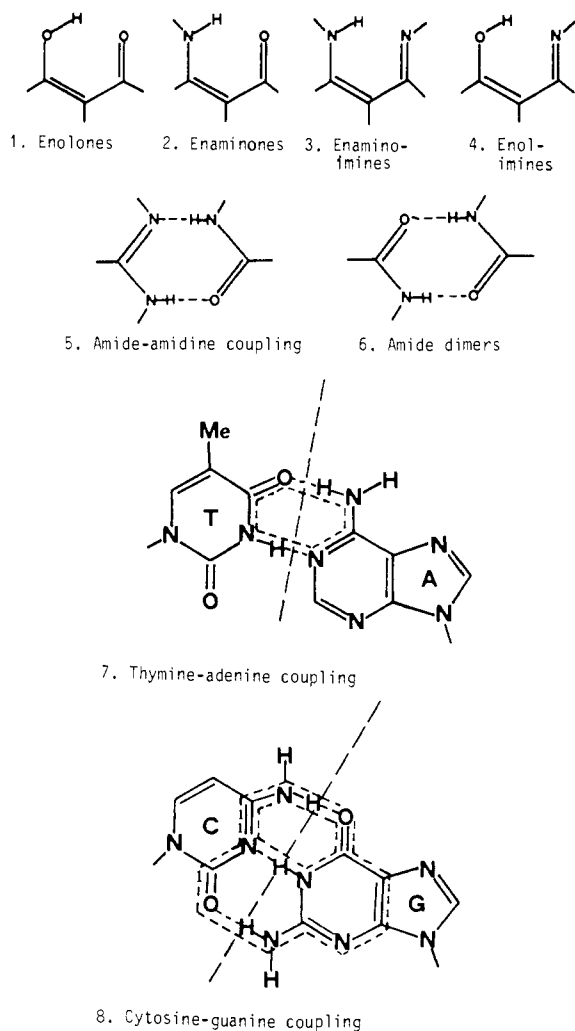
(22) Tayyari, S. F.; Zeegers-Huyskens, Th.; Wood, J. L. *Spectrochim. Acta* **1979**, *35A*, 1265.

(23) (a) Karlström, G.; Wennerström, H.; Jönsson, B.; Forsen, S.; Almlöf, J.; Roos, B. *J. Am. Chem. Soc.* **1975**, *97*, 4188. (b) Isaacson, A. D.; Morokuma, K. *J. Am. Chem. Soc.* **1975**, *97*, 4453. (c) Karlström, G.; Jönsson, B.; Roos, B.; Wenneström, H. *J. Am. Chem. Soc.* **1976**, *98*, 6851. (d) Bouma, W. J.; Vincent, M. A.; Radom, L. *Int. J. Quantum Chem.* **1978**, *14*, 767. (e) Fluder, E. M.; de la Vega, J. R. *J. Am. Chem. Soc.* **1978**, *100*, 5265. (f) George, P.; Bock, C. W.; Trachtman, M. *J. Comput. Chem.* **1980**, *1*, 373. (g) Bicerano, J.; Schaefer, H. F., III; Miller, W. H. *J. Am. Chem. Soc.* **1983**, *105*, 2550.

(24) Frisch, M. J.; Scheiner, A. C.; Schaefer, H. F., III; Binkley, J. S. *J. Chem. Phys.* **1985**, *82*, 4194.

(25) Huzinaga, S. *J. Chem. Phys.* **1965**, *42*, 1293. Dunning, T. H. *J. Chem. Phys.* **1970**, *53*, 2821.



**Chart I.** Some Molecular Fragments Which Are Known or Are Supposed To Be Involved in RAHBs

due to resonance  $\Delta E_{\text{RAHB}} = 36.9 \text{ kJ mol}^{-1}$ . The total hydrogen bonding energy is calculated with this model to be  $16.5 \text{ kJ mol}^{-1}$  for ice (in agreement with the usually reported value of some  $20 \text{ kJ mol}^{-1}$ ) and  $53.4 \text{ kJ mol}^{-1}$  for acetylacetone, which fits the already quoted *ab initio* value<sup>24</sup> of  $48.5\text{--}51.8 \text{ kJ mol}^{-1}$  for malonaldehyde and its average experimental value, which has been reported<sup>2</sup> to be some  $50 \text{ kJ mol}^{-1}$ . The barrier to proton transfer is calculated to be  $51.0 \text{ kJ mol}^{-1}$ , which is reduced to  $34.8 \text{ kJ mol}^{-1}$  by subtracting the zero-point energy of the fundamental state [one half of the  $\nu(\text{OH})$  stretching frequency of  $2700 \text{ cm}^{-1}$ ].<sup>2,19</sup> This value is probably too high and greater than the "best" *ab initio* value of  $18 \text{ kJ mol}^{-1}$  already quoted,<sup>24</sup> but it has to be noted that values in the range  $15\text{--}43 \text{ kJ mol}^{-1}$  have been calculated at different levels of theory. Recently<sup>13</sup> the molecular structure of acetylacetone has been determined by accurate gas-phase electron-diffraction methods and the  $Q$  and  $\lambda$  parameters and  $r = d_{\text{O-H}}$  and  $R = d_{\text{O}\cdots\text{O}}$  distances have been found to be  $-0.124$  and  $0.69$  and  $1.049$  ( $15$ )  $\text{\AA}$  and  $2.512 \text{ \AA}$ , respectively. The corresponding point is indicated by a star on the map of Figure 4, and it is seen

to correspond reasonably well to the minimum position on the map itself.

The experimental geometries of Table II are reported in Figure 4 as well (full points). All of them are located inside the almost diagonal energy valley and, as far as the causes of their exact position are concerned, two specific factors may be discerned. The first is of electronic nature, as very strong hydrogen bonds are associated only with fragments where the  $\beta$ -keto enolic fragment is the only conjugated system. The second effect is steric. All of the strongest hydrogen bonds are associated with bulky  $R_1$  and  $R_3$  substituents, and the clearest evidence comes from the comparison of compounds **19** and **11**, where the substitution of a methyl by a *tert*-butyl group reduces  $d_{\text{O}\cdots\text{O}}$  from  $2.665$  to  $2.552 \text{ \AA}$ . This fact is in agreement with the energy values calculated by introducing in eq 1 the  $E_{\text{vdw}}$  term corresponding to the van der Waals interactions of two *tert*-butyl groups in  $R_1$  and  $R_3$ , which shifts ( $r, R$ ) to  $(1.11, 2.48) \text{ \AA}$  and increases  $\Delta E_{\text{RAHB}}$  to  $45.5 \text{ kJ mol}^{-1}$  and the total hydrogen bond energy to  $82.5 \text{ kJ mol}^{-1}$  while the proton transfer barrier decreases to  $27.5 \text{ kJ mol}^{-1}$ .

### Conclusions and Generalization

The comparative analysis of all of the available crystal structures containing the acacH  $\beta$ -diketone fragment in its enol form seems to indicate that the intramolecular hydrogen bond (2) found in these compounds belongs to a specific type we have called RAHB as it is strengthened by the interplay with the conjugated  $\pi$ -bond system of the fragment. Moreover, a simple mathematical treatment based on this model gives quite reasonable values for hydrogen bond energies, confirming the reliability of the model itself at least in the intramolecular case. The RAHB model can be generalized by saying that "the interplay between hydrogen bond and heterodienes (or more generally heteroconjugated systems) can strengthen remarkably the hydrogen bond itself". A collection of molecular fragments which may be implied in this phenomenon via intermolecular (including dimerization) or intramolecular hydrogen bond formation is shown in Chart I, out of which enolones (1) are the object of the present study and preliminary data confirming the strong  $\pi$  delocalization of hydrogen-bonded enaminones and amino alcohols have been already reported.<sup>34</sup> Possible biochemical and biological implications originate from the fact that both thymine-adenine (7) and cytosine-guanine (8) couples in DNA are linked by two hydrogen bonds which reproduce the amide-amidine coupling (5) and that cytosine-guanine coupling implies another much wider cycle of hydrogen bonds and conjugated double bonds. Similar considerations can be made in connection with the hydrogen bonds determining the secondary structure of proteins as  $\alpha$ -helices contain three nearly parallel and isooriented  $\text{C}=\text{O}\cdots\text{HNC}=\text{O}\cdots\text{HN}$  chains of  $\pi$  heteroconjugated systems connected by hydrogen bonds and  $\beta$ -pleated sheets of infinite antiparallel arrays of identical chains.

**Acknowledgment.** We express our sincere appreciation to the referees for their helpful, constructive advice.

**Supplementary Material Available:** Tables of interatomic distances, structures, and internuclear angles and a plot of  $d_{\text{O-H}}$  and  $d_{\text{H}\cdots\text{O}}$  vs  $d_{\text{O}\cdots\text{O}}$  (6 pages). Ordering information is given on any current masthead page.

(34) Ferretti, V.; Bellucci, F.; Bertolasi, V.; Gilli, G. Proceedings of the IX ECM, Torino, Italy, 1985; p 337.